

2-D electrical resistivity imaging for investigating an active landslide along a ridgeway in Burdur region, southern Turkey

Sedat Yılmaz · Ceyda Narman

Received: 4 March 2014 / Accepted: 31 March 2014 / Published online: 13 April 2014
© Saudi Society for Geosciences 2014

Abstract Two-dimensional (2-D) electrical resistivity imaging (ERI) technique has been used to characterize a landslide which occurred in a ridgeway between Burdur and Isparta in southern Turkey. The problems related to this road showed an increase due to road constructions and heavy rainfall. Primary attention was drawn to the determination of the thickness of the mobilized material, its possible sliding surface, and evaluation of the groundwater conditions related to the occurrence of the landslide. The eight survey profiles in the landslide area were implemented. Electrical resistivity survey has been carried out by the Wenner–Schlumberger array for data acquisition and smoothness-constrained least-squares method for data inversion. The self-potential (SP) survey data are presented as one-dimensional profile for each of the lines. ERIs pointed out a great heterogeneity of the near surface or mobilizing material and presence of impermeable material that could be associated to lateral and vertical limits of permeability. SP anomalies displayed that the positive values were located in water discharge on the surface whereas negatives in the sites of infiltration. The sliding surface is at a depth of about 10 m.

Keywords Resistivity · Self-potential · Landslide · Wenner–Schlumberger

Introduction

Landslides, defined as the movement of a mass of rock, debris, or earth down a slope, are earthflows that can be triggered by a

variety of external factors. The most important causes of landslides in southern Turkey are, generally, morphology of slopes, heavy rainfall, excavation, decomposed rocks, and existence of underground water in soil material (Atayeter 2004).

Direct investigations to determine landslide characteristics by using geotechnical methods along with borehole data provides only the well data; however, the high cost of such methods implies that they are not always suitable (Jomard et al. 2007; Lee et al. 2008). Alternatively, geophysical surveys provide detailed information about landslide anatomy and provide new facilities for immediate survey of enormous areas at a relatively low cost (Bogoslovsky and Ogilvy 1977). Geophysical methods are noninvasive, in general, and the results can be transformed into the geotechnical means and produce crucial results in the investigation of landslide areas (Cosenza et al. 2006). The main objectives of geophysical surveys in mass movement or landslide areas are to define thickness and lateral extension of mobilized material, to determine potential sliding surfaces, and to ascertain of the movement of groundwater flow and its distribution within the slip mass (e.g., Carpentier et al. 2012; Chambers et al. 2011; Grandjean et al. 2011; Hibert et al. 2012).

By considering the local geological and structural setting and the type of mass movement, a careful selection of more than one geophysical method is particularly necessary and important to provide physical property information rather than direct geological or geotechnical data (Sastry and Mondal 2013). The two-dimensional (2-D) electrical resistivity imaging (ERI) and the self-potential (SP) techniques from the geophysical methods are the focus of this study.

The 2-D ERI technique is both relatively cheap to give a continuous subsurface image and possible to measure the ground response along profiles in order to obtain imaging of

S. Yılmaz (✉) · C. Narman
Department of Geophysical Engineering, Engineering Faculty,
Süleyman Demirel University, 32260 Isparta, Turkey
e-mail: sedatyilmaz@sdu.edu.tr

C. Narman
e-mail: ceydanarman@hotmail.com

the subsurface. In addition, since ERI method is sensitive to the water content of layer, it is suitable to be used in landslide investigations (Friedel et al. 2006; Lapenna et al. 2005; Piegari et al. 2009; Yilmaz 2007). Multielectrode data acquisition systems for the 2-D ERI technique made it possible to use unconventional electrode array, in addition to the classical arrays, thereby enabling a large amount of simultaneous measurements to be taken for each injection point, thus significantly reducing time for data acquisition (Martorana et al. 2009).

The SP technique involves the measurement of naturally occurring geoelectrical fields that are generated in the subsurface by a range of mechanisms and can be found in the related literature in detail (Telford et al. 1990). The use of SP in landslide studies is concerned primarily with electrofiltration or streaming potentials that are caused by the movement of fluid through porous rocks and soils (Revil et al. 1999). Furthermore, the objective of the use of this method is to identify zones negative and positive charges in landslide areas (Colangelo et al. 2006).

The aim of this study is to characterize a landslide occurred in a ridgeway between Burdur and Isparta in southern Turkey using 2-D ERI technique. SP profiling was also used in describing the main pattern of the subsurface fluid flows.

Physiography and geology

The study area is located 4 km from the Askeriye district of the province of Burdur in the Mediterranean region of southern Turkey (Fig. 1). Due to increasing traffic load and as a precaution to decrease traffic congestion in the coming years, a road-widening work was performed in this ridgeway route in the years of 2006 and 2009. Because of both widening and heavy rainfall except for negative lithology, this mass movement was formed along a hill-slope over the ridgeway (Fig. 2). Therefore, the current conditions threaten local traffic safety because of local degradation of the slope and slipping. This

landslide showing an inclination of about 18° has 130-m long and 110-m wide for the first failure zone and 75-m long and 55-m wide at the second failure zone (Fig. 3).

In the area, the Kayikoy Formation, Burdur Formation, and alluvium, autochthonous units, and the Gokcebag Complex and Akdag Limestone, allochthonous units, were observed (Sener et al. 2005) (Fig. 4). The Gokcebag ophiolitic complex is formed of limestone, diabase, serpentine, peridotite, gabbro, radiolarite, and chert series. The emplacement age of the complex is Late Lutetian. The complex was also described as an impermeable unit. The Akdag Limestone is located as an olistolith within the Gokcebag Complex. The Burdur Formation is composed of a marl, claystone, mudstone, and weakly cemented sandstone with tuff, tuffite, and travertine and is Pliocene in age. A Quaternary age unit was described as alluvium. The unit consists of gravel, sand, clay, and silt, which are loosely cemented. The Kayikoy Formation, exposing at the landslide area, consists of sedimentary rock sequences, components of which are sandstone, conglomerate, shale, clayey limestone, and cherty limestone. It was deposited as a flysch facies of Upper Paleocene–Medium Eocene age. The formation, representing the flysch properties, was described as an impermeable unit. The basement is composed of the yellowish-gray colored micritic-textured clayey limestone and overlying materials comprising yellowish-gray medium-layered sandstone, claystone, and polygenic gravelly conglomerate slips over it.

Data acquisition and process

The entire site of a landslide, occurred in a ridgeway between Burdur and Isparta in southern Turkey, was studied along eight profiles using 2-D ERI method (Fig. 5). To describe the main pattern of the subsurface fluid flows in landslide area, SP profiling was also used in five lines. A brief description of two techniques as applied to this study follows.

The 2-D ERI data in an environment with an altitude ranging from 1,137 to 1,185 m (Fig. 5) were collected at landslide area during December 2012. All data were acquired using a multichannel resistivity meter by GF Instruments. A maximum of 48 electrodes were used for each layout, with an electrode spacing of 4 m. Wenner–Schlumberger array surveying was employed. This array type was chosen because it generally provides higher signal levels for deeper measurements and is more sensitive to resistivity variations with depth (Dahlin and Zhou 2004; Loke 2013). Five 2-D ERI (P1 to P5) with lengths of 188 m were performed in east–west direction, two (P6 and P7) in north–south direction, and one (P8) in southeast–northwest direction. Resistivity data sets were inverted using a smoothness-constrained least-squared inversion software (RES2DINV version 3.56) using a quasi-Newton technique to reduce calculations (Loke and Barker 1996; Loke et al. 2003). The inversion program is a forward

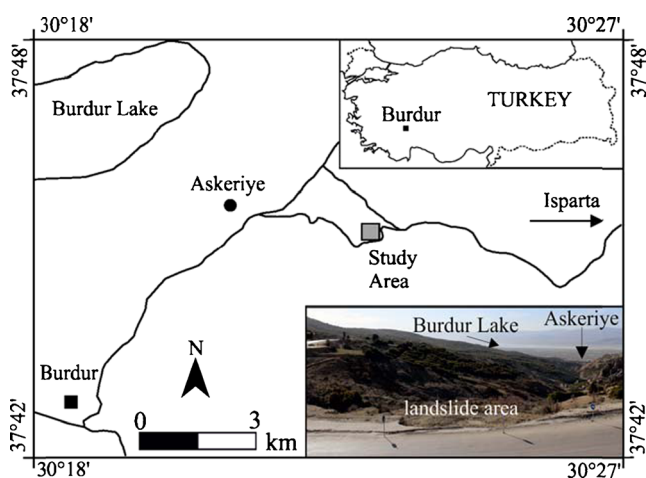
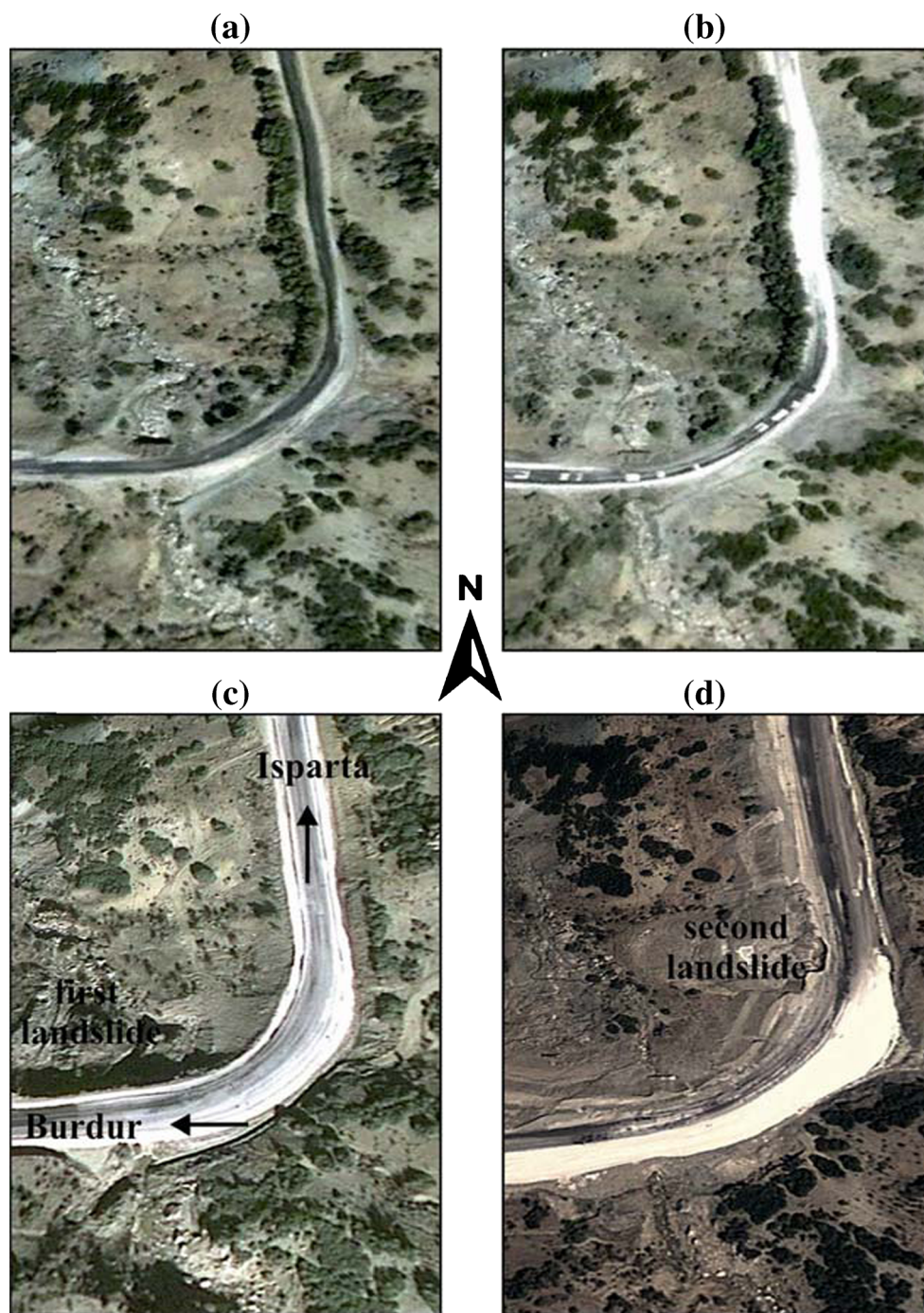


Fig. 1 A map showing the location of the study area, and a scenic view of the site showing the landslide area

Fig. 2 Identification of landslide occurrence associated with the road-widening works based on aerial photographs by years 2003 (a), 2006 (b), 2009 (c), and 2011 (d)



modeling method consisting of a number of rectangular blocks, block arrangement being loosely tied to data distribution in the pseudo-section. The forward modeling subroutine was used to calculate apparent resistivity values, and a non-linear least-squares optimization technique was used for the inversion routine (Loke and Barker 1996). The root mean square (RMS) is a measure of its fitness between measured apparent resistivities and the apparent resistivities of the model response from the inverted resistivity (Loke and Barker 1996).

SP data were undertaken along profiles occupying the five lines (P1 to P5) used for 2-D ERI surveys. The separation between measurement points along the five lines was 5 m. The SP data acquisition with the fixed-base (or total field) was achieved with a millivoltmeter and a pair of nonpolarizable electrodes. The reference electrode was established at a fixed point, and the roving electrode was moved across the survey area to the prepared positions; at each survey point, the potential difference between the electrodes was recorded. The

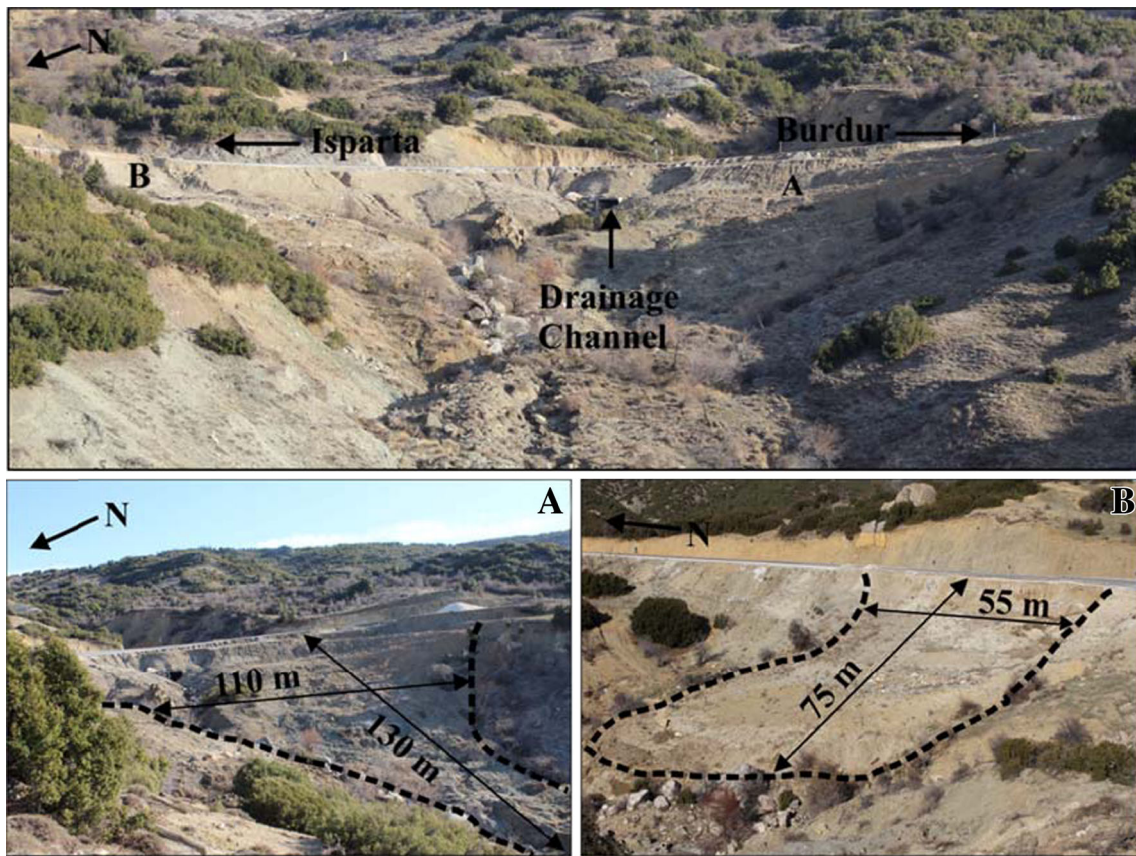


Fig. 3 A photo of the survey site, taken from the opposite (NW) side of the highway (top). A and B denotes different parts of landslide scarp. Views of the first (a) and second (b) failure zones (bottom)

SP values in measuring net have been obtained by adding readings after establishing a SP arbitrary zero value as a point of reference in the area. The SP measurements have been corrected in order to compensate for cumulative errors, by distributing linearly the closure errors along each circuit. In order to obtain a better view of the SP anomalies, we have subtracted the net average value of all SP data from the potential in each point. Finally, we obtained graphs for each of the lines using a one-dimensional drawing.

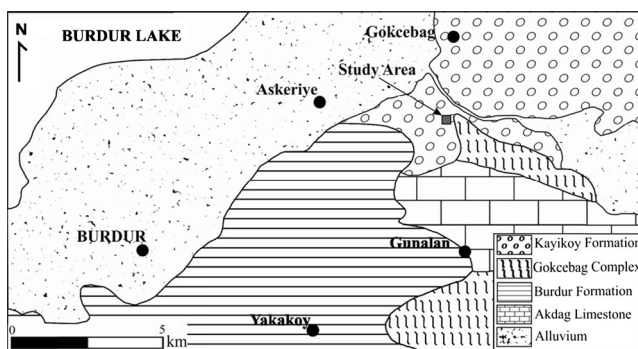


Fig. 4 Surface geology map of the Burdur area (modified after Sener et al. (2005))

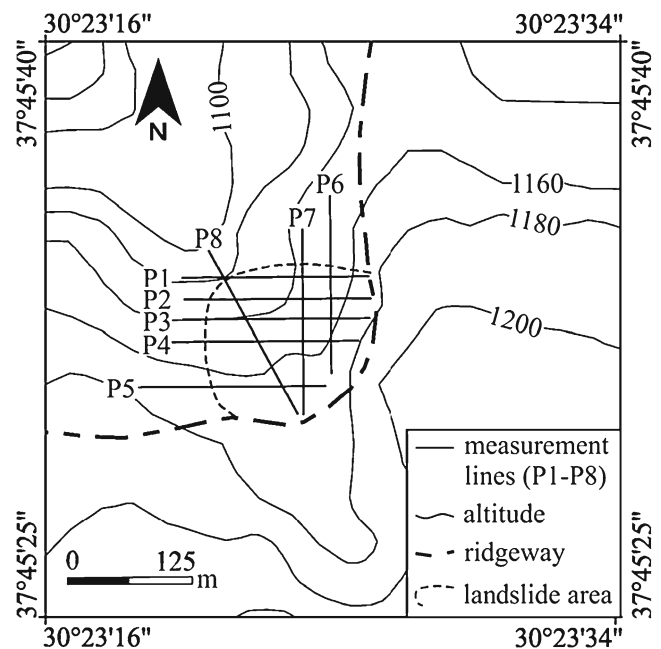


Fig. 5 Location of the measurement lines; eight ERI (P1 to P8) and five SP survey profiles (P1 to P5) were performed in the east–west or west–east (E–W or W–E), north–south (N–S), and northwest–southeast (NW–SE) directions

Results and discussion

To detect subsurface geometry with the Wenner–Schlumberger array, eight 2-D ERIs were carried out in the landslide area (Figs. 6, 7, and 8). Five SP profiling measurements were also carried out to describe the main pattern of the subsurface fluid flows (Figs. 6 and 7). The inversion results of all 2-D ERI profiles indicated that the depth of penetration varies between 27 and 35 m. In all cases, the number of iterations has varied between 3 and 5 with root mean square (RMS) errors ranging from 2.9 to 15.8 %. A preliminary inspection of the obtained resistivity images allows identifying a small range of resistivity values (3–80 Ωm) indicating a weak discontinuity in the electrical properties.

The 2-D inverted resistivity sections and SP profiling graphs from survey profiles P1 to P3 performed in the east–west direction are shown in Fig. 6. In all cases, the numbers of iterations for the ERI sections are 5, 5, and 3 with RMS values 10.0, 6.3, and 15.8 %, respectively. The 2-D ERI sections pointed out either slide characteristics or the material uninvolved in the movement. All the 35-m deep ERI sections show the same distribution as the resistivity values. The shallow high resistivity layer (>20 Ωm) at near surface of the E side of the ERIs correspond to the mobilizing material. The deepest part of the ERIs shows very conductive values (2 to 10 Ωm) corresponding to impermeable material associated either with clayey material not involved in the slide or higher water content. The central part of the P1 to P3 images is characterized by a resistive material (20–80 Ωm) near the surface with a lenticular shape that could be associated with toe of the slope suppressing the slide. The near surface high resistivity values (>20 Ωm) at the right side of the drainage path at the central part of the ERIs reflect the mobilizing material and lateral limits of the first landslide. The high resistive values (>20 Ωm) at the W side of ERIs show the material uninvolved in the movement. The positive SP down-slope is consistent with a streaming potential signature produced by infiltration at accumulation at the base corresponding toe for landslide at positions between 75 and 110 m in the ERI sections in Fig. 6. Positive charges are carried in the direction of the fluid flow, producing positive SP anomalies on the surface, where water discharge is located, and negative in the sites of infiltration.

The 2-D inverted resistivity sections and SP profiling graphs from survey profiles P4 and P5 performed in the west–east direction are shown in Fig. 7. The numbers of iterations for the ERI sections are 5 and 4 with RMS values 4.4 and 6.4 %, respectively. The profile P4 (Fig. 7a) pointed out high resistivity values (>20 Ωm) at near surface of the E side of the image corresponding to the mobilizing material of the first landslide. The lower resistivity zone (<10 Ωm) at position 95 m is due to drainage path. The deepest part of the E side and at near surface of the W side of image show very conductive values (2 to 10 Ωm) corresponding to impermeable zone associated either with clayey material not involved in the slide or higher water content. The profile P5 (Fig. 7b) pointed out high resistivity values (>20 Ωm) between near surface of the W side and position 125 m of image and the impermeable material in the deepest part of the section. The positive SP values at the middle of P4 and at the end of P5 are due to the water discharge from the drainage channel and path eventuated the low resistivities (<10 Ωm) at positions 95 and 145 m in ERI sections, respectively. The negative SP values at the west side of SP profiles also display the sites of infiltration in the other slope to be thought as potential landslide zone.

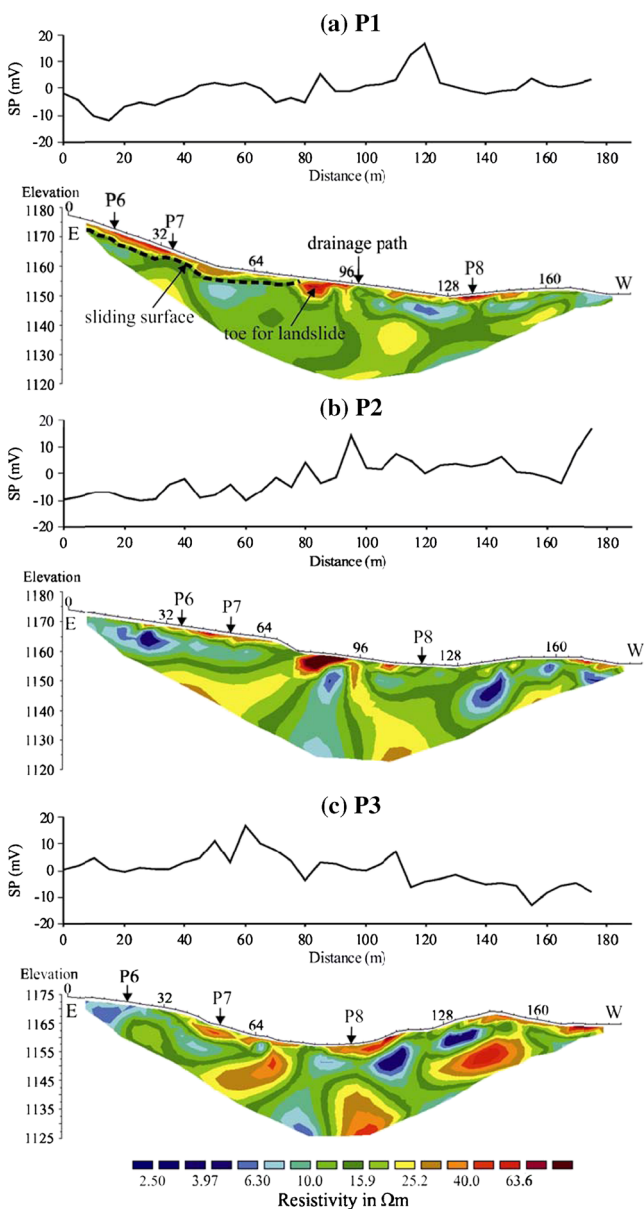


Fig. 6 The 2-D inverted resistivity sections and SP anomalies from profiles P1 (a), P2 (b), and P3 (c) in the E–W direction

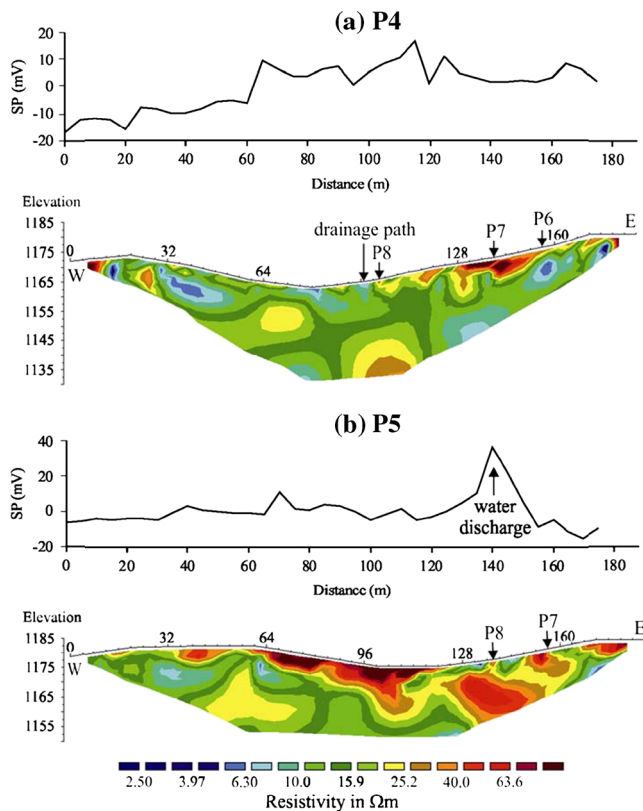


Fig. 7 The 2-D inverted resistivity sections and SP anomalies from profiles P4 (a) and P5 (b) in the W–E direction

The 2-D inverted resistivity sections from survey profiles P6 to P8 are shown in Fig. 8. In all cases, the numbers of iterations for the ERI sections are 3, 5, and 4 with RMS values 13.0, 5.3, and 2.9 %, respectively. The profiles P6 and P7 performed in the north–south direction pointed out high resistivity values ($>20\Omega\text{m}$) corresponding to the mobilizing material of the landslide at near surface of the images. The lower resistivity zone ($<10\Omega\text{m}$) under the landslide material is due to impermeable zone associated either with clayey material not involved in the slide or higher water content. The deepest and near surface of the N side of images show the higher resistive values ($>20\Omega\text{m}$) corresponding to the inactive zone. The lateral limit of landslide is near the profile P1, and the sliding surface is at a depth of about 10 m. The profile P8 performed in the northwest–southeast direction, longitudinal to the landslide body, pointed out a great heterogeneity of the near surface or mobilizing material and presence of impermeable material that could be associated to lateral and vertical limits of permeability that could affect the groundwater pathway and circulation of the slope (Fig. 8c). The ERI section, with a penetration depth of about 35 m, shows that the high resistivity values ($>20\Omega\text{m}$) for the first 10 m of subsurface, corresponding to the mobilizing material of the first landslide, were detected near the surface at positions 24–166 m. The lower resistivity values ($<20\Omega\text{m}$) in the deepest part,

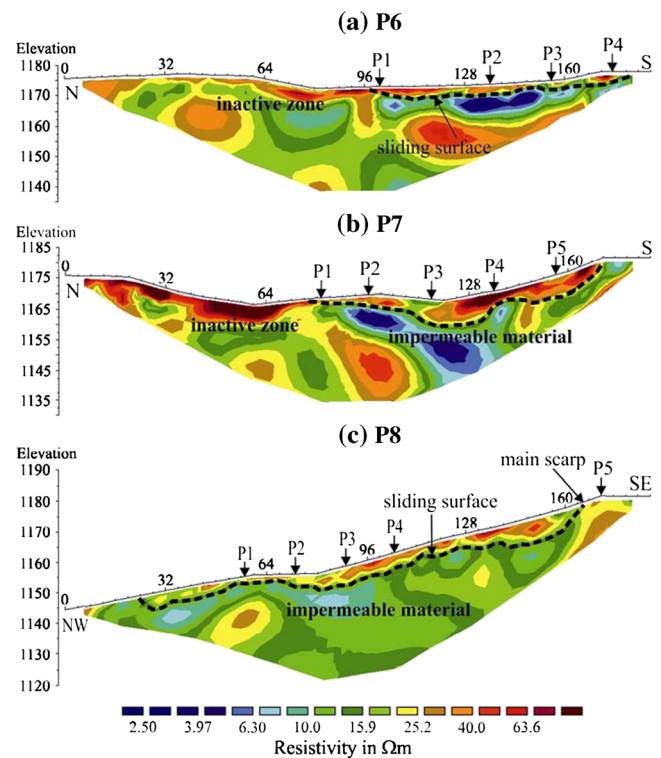


Fig. 8 The 2-D inverted resistivity sections from profiles P6 (a) and P7 (b) in the N–S direction and P8 (c) in the NW–SE direction

corresponding to the impermeable zone, could be related to clayey material or higher water content.

Conclusions

2-D ERI investigation has been performed to investigate a landslide which occurred along the Burdur–Isparta ridgeway in the Mediterranean region of southern Turkey. The high resolution of the ERIs reveals the sliding surface and the thickness of the landslide material. The SP technique allows relevant results in describing the main pattern of the subsurface fluid flows and delineating the boundaries of the landslides.

ERIs pointed out a great heterogeneity of the near surface or mobilizing material and presence of impermeable material that could be associated to lateral and vertical limits of permeability. The high resistivity values ($>20\Omega\text{m}$) for the first 10 m of subsurface and the lower resistivity values ($<20\Omega\text{m}$) in the deepest part could be related to the mobilizing material and the impermeable zone of the landslide, respectively. The SP anomalies display increasingly positive values from the top of the slope to the base. The positive SP values are located in water discharge on the surface and the negative values in the sites of infiltration. The integrated interpretation of the 2-D ERI and SP profiles deduce that the trend of increasingly positive SP values is discontinued at the front of drainage path and at the accumulation zone or toe for landslide (see Figs. 6

and 7). At these locations, surface discharge of water was observed; the former being related to seepages directly from landslide material.

The ERIs revealed the sliding surface at a depth of about 10 m. This landslide study would be used for a stability assessment of the area for foreseeable future the studies.

Acknowledgments Financial support by the Süleyman Demirel University Research Fund is gratefully acknowledged. The authors would like to thank to the anonymous reviewers for their constructive comments which have helped to improve this manuscript.

References

- Atayeter Y (2004) Landslides on the ridgeway between Gelincik (Isparta)-Askeriye (Burdur) villages. *Burdur J Educ Fac* 8:17–31
- Bogoslovsky VA, Ogilvy AA (1977) Geophysical methods for the investigation of landslides. *Geophysics* 42:562–571
- Carpentier S, Konz M, Fischer R, Anagnostopoulos G, Meusburger K, Schoeck K (2012) Geophysical imaging of shallow subsurface topography and its implication for shallow landslide susceptibility in the Urseren Valley, Switzerland. *J Appl Geophys* 83:46–56
- Chambers JE, Wilkinson PB, Kuras O, Ford JR, Gunn DA, Meldrum PI, Pennington CVL, Weller AL, Hobbs PRN, Ogilvy RD (2011) Three-dimensional geophysical anatomy of an active landslide in Lias Group mudrocks, Cleveland Basin, UK. *Geomorphology* 125:472–484. doi:10.1016/j.jappgeo.2012.05.001
- Colangelo G, Lapenna V, Perrone A, Piscitelli S, Telesca L (2006) 2D Self-Potential tomographies for studying groundwater flows in the Varco d'Izzo landslide (Basilicata, southern Italy). *Eng Geol* 88:274–286
- Cosenza P, Mannet E, Rejiba F (2006) Correlations between geotechnical and electrical data: a case study at Garchy in France. *J Appl Geophys* 60:165–178. doi:10.1016/j.jappgeo.2006.02.003
- Dahlin T, Zhou B (2004) A numerical comparison of 2D resistivity imaging with 10 electrode arrays. *Geophys Prospect* 52:379–398. doi:10.1111/j.1365-2478.2004.00423.x
- Friedel S, Thielen A, Springman SM (2006) Investigation of a slope endangered by rainfall-induced landslides using 3D resistivity tomography and geotechnical testing. *J Appl Geophys* 60:100–114. doi:10.1016/j.jappgeo.2006.01.001
- Grandjean G, Gourry JC, Sanchez O, Bitri A, Garambois S (2011) Structural study of the Ballandaz landslide (French Alps) using geophysical imagery. *J Appl Geophys* 75:531–542. doi:10.1016/j.jappgeo.2011.07.008
- Hibert C, Grandjean G, Bitri A, Travelletti J, Malet JP (2012) Characterizing landslides through geophysical data fusion: example of the La Valette landslide (France). *Eng Geol* 128:23–29. doi:10.1016/j.enggeo.2011.05.001
- Jomard H, Lebourg T, Tric E (2007) Identification of the gravitational boundary in weathered gneiss by geophysical survey: La Clapière landslide (France). *J Appl Geophys* 62:47–57. doi:10.1016/j.jappgeo.2006.07.003
- Lapenna V, Lorenzo P, Perrone A, Piscitelli S, Rizzo E, Sdao F (2005) 2D electrical resistivity imaging of some complex landslides in the Lucanian Apennine chain, southern Italy. *Geophysics* 70:11–18. doi:10.1190/1.1926571
- Lee CC, Yang CH, Liu HC, Wen KL, Wang ZB, Chen YJ (2008) A Study of the hydrogeological environment of the lishan landslide area using resistivity image profiling and borehole data. *Eng Geol* 98:3–4. doi:10.1016/j.enggeo.2008.01.012
- Loke MH (2013) Tutorial: 2-D and 3-D electrical imaging surveys. <http://www.geotomosoft.com>. Accessed 24 June 2013
- Loke MH, Barker RD (1996) Rapid least-squares inversion of apparent resistivity pseudosections by a quasi-Newton method. *Geophys Prospect* 44:131–152. doi:10.1111/j.1365-2478.1996.tb00142.x
- Loke MH, Acworth I, Dahlin T (2003) A comparison of smooth and blocky inversion methods in 2-D electrical imaging surveys. *Explor Geophys* 34:182–187
- Martorana R, Fiandaca G, Ponsati AC, Cosentino PL (2009) Comparative tests on different multi-electrode arrays using models in near-surface geophysics. *J Geophys Eng* 6:1–20. doi:10.1088/1742-2132/6/1/001
- Piegari E, Cataudella V, Di Maio R, Milano L, Nicodemi M, Soldovieri MG (2009) Electrical resistivity tomography and statistical analysis in landslide modelling: a conceptual approach. *J Appl Geophys* 68:151–158. doi:10.1016/j.jappgeo.2008.10.014
- Revil A, Pezard PA, Glover PWJ (1999) Streaming potential in porous media. 1. Theory of the zeta potential. *J Geophys Res* 104:20021–20031
- Sastry RG, Mondal SK (2013) Geophysical characterization of the Salna Sinking Zone, Garhwal Himalaya, India. *Surv Geophys* 34:89–119. doi:10.1007/s10712-012-9206-y
- Sener E, Davraz A, Ozcelik M (2005) An integration of GIS and remote sensing in groundwater investigations: a case study in Burdur, Turkey. *Hydrogeol J* 13:826–834. doi:10.1007/s10040-004-0378-5
- Telford WM, Geldart LP, Sheriff RE (1990) *Applied geophysics*, Second Edition edn. Cambridge University Press, Cambridge
- Yilmaz S (2007) Investigation of Gürbulak landslide using 2D electrical resistivity image profiling method (Trabzon, northeastern Turkey). *J Environ Eng Geophys* 12:199–205. doi:10.2113/JEEG12.2.199